August 27-31, 2023
FLORENCE - ITALY

ICWE 16

16th International
Conference on
Wind Engineering

Towards improvement of wind resistance and ventilation for layout of buildings using urban LES data

Masaharu Kawaguchi [1], Tetsuro Tamura [2], Masaru Yoshikawa [3]

[1]*Tokyo Institute of Technology, Tokyo, Japan, kawaguchi.m.ag@m.titech.ac.jp*
[2]*Tokyo Institute of Technology, Tokyo, Japan, tamura.t.ab@t.titech.ac.jp*
[3]*Taisei Corporation, Yokohama, Japan, masaru.yoshikawa@sakura.taisei.co.jp*

SUMMARY:
A comprehensive numerical assessment of the wind resistance and ventilation performance of an actual urban area was carried out in a few urban transformation cases and ventilation characteristics for each case was discussed based on the streamlines, breathability and distribution of wind speed statistics. In the high-rise redevelopment scenario, a clear decrease in wind safety was predicted, along with improved ventilation performance. In the alternative redevelopment cases, the proposed low- to mid-rise urban block geometries enhanced near-ground ventilation, restraining intense gusts occurrence. The result also showed the importance of considering the prevailing wind direction in urban planning.

Keywords: LES, urban ventilation, wind resistance

1. INTRODUCTION
In recent years, many urban redevelopment projects have been emphasizing environmental and disaster prevention performance. As a result of urban intensification and climate change, many cities have been experiencing deterioration of wind safety and comfort as well as thermal conditions. Improving ventilation performance is one effective means of enhancing the quality of the urban environment, but this is often a trade-off for the risk of high wind damage. Therefore, ventilation assessment and wind resistance assessment should be carried out simultaneously.

There are several perspectives for ventilation assessment. Neophytou and Britter (2005) proposed a concept of breathability for horizontal homogeneous cities by defining it as the ability to exchange the air flow below and above the canopy region. Recently, similar breathability analyses were performed based on the vertical kinetic energy flux and ventilation mechanism was discussed (Ogihara et al., 2022). On the other hand, in dense high-rise urban areas, the flow easily becomes stagnant, and pollutants accumulate in under-ventilated spaces. Thus, the flow pattern needs to be designed to use both horizontal flow and vertical air exchange effectively. This paper presents a comprehensive numerical assessment of ventilation and wind resistance for various city block models of possible urban transformation by using breathability and mean wind and peak gust speed for evaluation indicators.

2. PROBLEM FORMULATION
2.1 Numerical Simulation
LES of the urban area was performed with a unified fluid-structure simulation framework called CUBE (Jansson et al., 2019). The programme is highly parallelised and has good load-balancing performance owing to the multi-block hierarchical cartesian grid system and immersed boundary method for complex geometry. The accuracy of the CUBE for wind engineering applications was validated by Cao et al. (2019). The inflow turbulence was prepared by LES using the quasi-periodic boundary condition by Nozawa and Tamura (2001), and a typical turbulence profile over urban areas

was reproduced (power-law index $\alpha = 0.20$). The minimum grid resolution was about 90 cm, and the total grid number was around 400 million. For spatial discretisation, the second-order central difference was adopted and 5% first-order upwind difference was mixed for the convection term. Further investigation on the effects of numerical viscosity is required. Time integration was performed by the Crank-Nicolson method. Dynamic Smagorinsky model is adopted for sub-grid turbulence stress terms. We performed the simulation with a 1:400 scale model. The breadth of the target building model is 0.175 m, inflow speed 7.7 m/s and viscosity 1.83×10^{-5} Pa·s. The approximate Reynolds number is 8.9×10^4. Due to complex ground surface, the flow becomes very unsteady and fluctuates spatially. Accordingly, the numerical stability is maintained. We converted the result to full scale for assessment, assuming the mean inflow speed at the actual target building height (224 m) is 36.0 m/s for the wind resistance assessment and 5.6 m/s (corresponding to 3.0 m/s at 10 m) for the ventilation assessment.

2.2. Case Overview

In this study, an actual low- to mid-rise block in a dense urban area in Tokyo was selected (Case 0 or C0), which is an example of neighbourhoods surrounded by taller buildings built in later years. It was transformed into three different arrangements of equivalent volume, as shown in Figure 1. In Case 1 (C1), the urban block was replaced by a single high-rise building, as is the case of typical conventional urban redevelopment projects. In Case 2 (C2) and Case 3 (C3), the urban block was replaced with a multi-building block which comprises several rectangular low-rise and mid-rise buildings, intending to facilitate vertical air exchange. The long sides of the mid-rise buildings were aligned orthogonal to the wind direction in Case 2, whilst it was set parallel in Case 3. Buildings and topography within a radius of 600 m from the target area were replicated in this simulation.
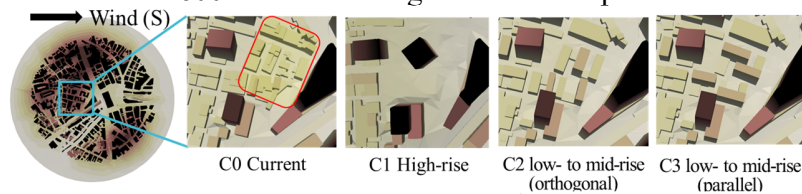

Wind (S)

C0 Current   C1 High-rise   C2 low- to mid-rise (orthogonal)   C3 low- to mid-rise (parallel)

Figure 1. Case Overview

2.3 Evaluation Method

Ventilation performance was evaluated based on breathability and mean wind speed, while 3-s peak gust speed was utilized as evaluation indicator for wind resistance. As for breathability, we calculated it based on kinetic energy flux in the vertical direction. According to the transportation equations of kinetic energy, breathability can be expressed as a summation of the four different types of fluxes: advection of mean kinetic energy ($1/2 \langle u_i \rangle \langle u_i \rangle \langle u_3 \rangle$, MA), diffusion of mean kinetic energy ($1/2 \langle u_i \rangle \langle u_i"u_3"\rangle$; MD), advection of turbulent kinetic energy ($1/2 \langle u_i"u_i"\rangle \langle u_3 \rangle$; TA) and diffusion of turbulent kinetic energy ($1/2 \langle u_i"u_i"u_3"\rangle$; TD). The sign of the values indicates the direction of transportation. (Positive values mean transportation upward.) The ratio of these four components reflects the ventilation characteristics in each urban block shape. We analysed breathability at two different levels, i.e., the approximate canopy layer height (z ~ 45 m) and near-ground level inside the canopy layer (z ~ 15 m). Comparison was carried out for the same horizontal area (350 m × 200 m) inside the transformed urban block. Analysis was performed with the time sequential volume data equivalent to 10 min on full scale.

3. VENTILATION AND WIND RESISTANCE BASED ON NUMERICAL RESULTS
3.1 General Features of the Flow Field

First, we examined the general features of each simulation case by the average streamlines. The seeds of the streamlines were set just above the approximate canopy layer top. The colour of the lines represents altitude. In Case 0, most of the approaching flow skimmed over the urban block and very little air intruded in the near-ground region. In Case 1, descending contracted flow was created in the wide-open space around the tall buildings. Streamlines of Case 2 significantly by with building. Both lateral vortices and vertical swirls were generated at different heights and

locations. Strong downwash at the sides of the buildings was also observed. Meanwhile, in Case 3, only minor interference of the buildings was observed. The winds smoothly blew down the target block with a little undulation in height.
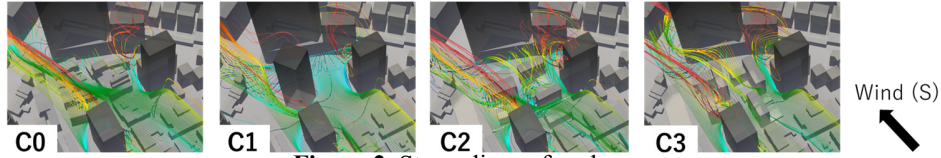

Figure 2. Streamlines of each case.

3.2 Ventilation Performance

Figure 3 (a) shows the integral of breathability and its four components over the inspection area at z ~ 45 m and z ~15 m for each simulation case. Note that up- and downward fluxes are separately integrated to avoid cancelling each other out. As for air intake at the top of the canopy layer, the breathability of Case 1 is by far the highest of all four cases and about 8 times higher than that of current case (Case 0). Differences among the other three cases are relatively small. In all four cases, energy was primarily transported by MA. In Cases 1 and 2, MD was the secondary factor, whereas TA followed MA in Cases 0 and 3. This may indicate that the field in Cases 1 and 2 are both more diffusive due to the generation of unsteady vortices. In the field in Case 0 and Case 3, vertical advection effect is more significant. Concerning air ejection at the canopy top, in all four cases, there are only small differences and both MA and MD contributed to the vertical flux. As for downward transportation at near-ground level, the breathability was significantly improved in Cases 1–3, namely 7.4 times, 2.9 times and 2.3 times higher than that of Case 0, respectively. In Cases 1–3, contribution of MD and TA to breathability was more substantial than in Case 0. Upward transportation of kinetic energy also increased at the near-ground level in Cases 1–3. The directions of net energy transportation in all cases but Case 1 were upward at the canopy top and downward at the near-ground level. In Case 1, it was opposite to the other cases. The imbalance between up- and downward fluxes was compensated by the flows passing the lateral boundaries. Figure 3 (b) shows the comparison of high-breathability regions between Case 2 and Case 3. In Case 2, those regions were formed by the target buildings altering the flow pattern around themselves. In Case 3, vertical air exchange was created in interaction with relatively large flow structures around the high-rise buildings.
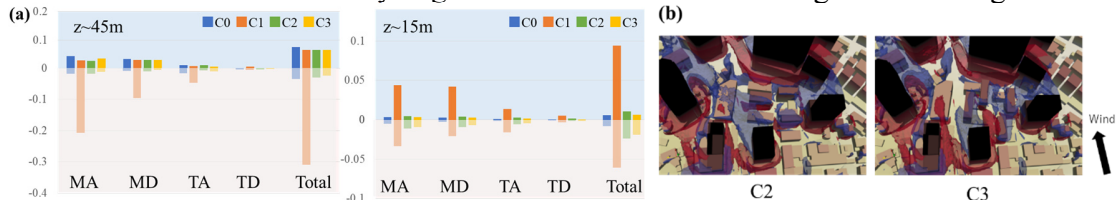

Figure 3. Breathability (a) integral over the inspection sections (b) iso-surface +1.6 m^3/s^3(blue), -1.6 m^3/s^3(red).

As a next step, we examined stagnant flow formation. Figure 4 (a) maps the distribution of mean wind speed at near-ground level (z~ 15 m), and Figure 5 (a) shows its frequency and less than cumulative frequency curves. In Case 0, very little air exchange exists near the ground. Velocity is generally low in streets orthogonal to the wind direction. We adopt the 50th percentile value of Case 0 (0.8 m/s) for the threshold of the under-ventilated area. In Case 1, owing to the space reserved around the buildings and the strong downwash of the high-rise buildings, the mean wind speed significantly increased and was higher than the thresholds almost everywhere. In Cases 2 and 3, the mean wind speed increased, and the low-ventilated areas were substantially reduced to 20 % of the whole inspection area. Spatial velocity variation was relatively large in Case 2, while wind speed uniformly increased across the area in Case 3. Also, relatively large noticeable under-ventilated spaces were formed in areas surrounded by buildings in Case 2.

3.3 Wind Resistance

Lastly, we examined strong gust occurrence in the target area based on the 3-s peak gust speed for

wind safety. Figure 4 (b) shows the distribution of the peak gust speed, and Figure 5 (b) shows its frequency and more than cumulative frequency curves. In Case 0, intense gusts over 20 m/s occurred in parts of streets parallel to the wind direction. In Case 1, peak gust speed exceeded 20 m/s almost everywhere. The average peak gust speed of the area reached twice the original value. In Case 2, the expansion of the area experiencing intense gusts due to contracted flow and downwash of mid-rise buildings were limited. In Case 3, gust generation in the target area was restrained in comparison with Case 0.
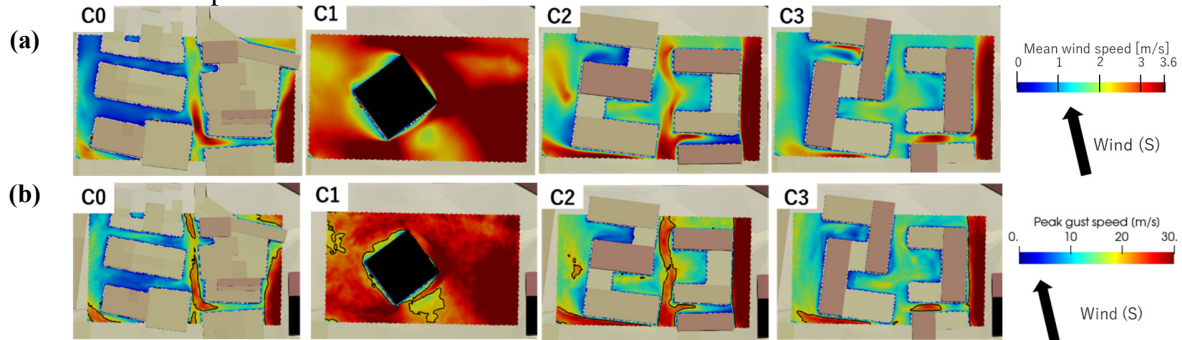
Figure 4. Wind speed map at z ~ 15 m. (a) mean wind speed (b) peak gust speed
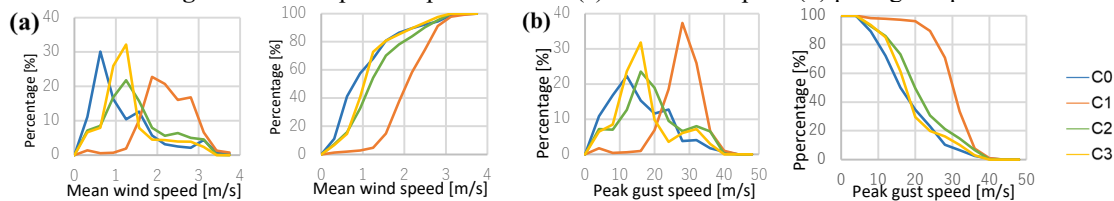
Figure 5. Frequency and cumulative frequency curves of wind speed at z ~ 15 m. (a) mean wind speed (b) peak gust speed.

4. CONCLUSION

A comprehensive numerical assessment for the transformation of an actual urban area was conducted regarding ventilation performance and wind resistance, and the following conclusion was obtained.

- High-rise buildings are highly effective for generating vertical air exchange at both the canopy top and near-ground levels. It also facilitated horizontal flow inside the canopy. However, the peak gust speed averagely doubled in the target area due to the intense downwash and shear layers formation. Thus, the wind resistance near the high-rise buildings can be significantly reduced.

- Two urban block geometries which comprises low and mid-rise buildings were tested. Breathability near the ground increased by 2.3–2.9 times, although it was not significantly altered at the canopy top. Pronounced differences in the flow pattern were observed depending on building orientation and indicated the effectiveness of consideration of the prevailing wind direction. When the long sides of the buildings were aligned parallel to the wind direction, the wind speed was distributed more uniformly without generating intense gusts.

REFERENCES
Cao, Y., Tamura, T., Kawai, H., 2019. Investigation of wall pressures and surface flow patterns on a wall-mounted square cylinder using very high-resolution Cartesian mesh, Journal of Wind Engineering and Industrial Aerodynamics 188, 1–18
Jansson, N., Bale, R., Onishi, K., Tsubokura, M., 2019. CUBE: A scalable framework for largescale industrial simulations. The International Journal of High Performance Computing Applications 33(4), 678–698.
Neophytou, M., Britter, R., 2005. Modelling the wind flow in complex urban topographies: a Computational-Fluid-Dynamics simulation of the central London area. 5th GRACM International Congress on Computational Mechanics, 967–974.
Nozawa, K., Tamura, T., 2001. Large eddy simulation of turbulent boundary layer over a rough ground surface and evaluation. Journal of Structural and Construction Engineering (AIJ) 501, 87–94. (Japanese)
Ogihara, R., Ishida, Y., Ono, Y., Mochida, A., 2022. Influences of high-rise building and non-uniformity of building height on city breathability. Summaries of technical papers of Annual Meeting, Architectural Institute of Japan, 40779. (Japanese)